DRUG DEVELOPMENT AND INDUSTRIAL PHARMACY, 20(15), 2353-2367 (1994)

SURFACE MORPHOLOGY STUDY OF SOLID POWDERS EVALUATED BY PARTICLE SIZE DISTRIBUTION AND NITROGEN ADSORPTION

Damrongsak Faroongsarng@ and Garnet E. Peck*
Department of Industrial and Physical Pharmacy
School of Pharmacy and Pharmacal Sciences
Purdue University, West Lafayette
IN 47907.

ABSTRACT

The surface morphology of five tableting excipients including unmilled dicalcium phosphate dihydrate (Di-Tab), microcrystalline cellulose (Avicel PH102), corn starch, croscarmellose sodium (Ac-di-sol), and sodium starch glycolate (Primojel) was studied using laser scattering particle size analysis and nitrogen adsorption surface area analysis. The surface area of particles disregarding porosity was obtained from the particle size distribution and the total area was obtained from the B.E.T. treatment of nitrogen adsorption results. The so-called Surface Irregularity Index (*SII*) was established to indicate surface roughness due to porosity. The *SII* value was consistent with the microscopic visualization of a powder sample. Furthermore, the nitrogen adsorption-desorption isotherm hysteresis which showed the evidence of porosity was also consistent with the index. The *SII* may be an alternative way to characterize the surface morphology of a solid powder.

@ recent address: Faculty of Pharmaceutical Sciences, Prince of Songkla University, Had Yai, Thailand 90112.
* To whom correspondence should be addressed.

INTRODUCTION

The surface properties of a solid could be characterized by particle size distribution and porosity (1). For instance, the specific surface of a solid powder could be determined by the geometry of particle sizes and size distribution (2). Dalla Valle, in 1943 (3), introduced the shape factor that related particle surface area to surface or volume mean particle diameter. The relationship was recently discussed in the literature (4). The shape factor values for some geometric shapes were also suggested (4). Theoretically, the specific surface of a system of particle size distribution having the true density (ρ) can be calculated as follows (2).

$$A = \frac{f}{\rho L} \frac{\sum(\nu_i \lambda_i^2)}{\sum(\nu_i \lambda_i^3)} \quad \text{.....(1)}$$

where ν_i is the ratio between number of particles falling in the i^{th} range of size having mean, l_i, and the total number of particles. The f and L are the shape factor and the most frequently occurring size, respectively. The mean size (l_i) is related to the most frequently occurring size (L) by a constant λ_i, i.e., $l_i = \lambda_i L$.

The surface area calculated from the size distribution could not represent the true specific surface because the surface area accounted for the porosity is disregarded. The currently applicable method of a powder's specific surface determination is nitrogen adsorption (5) using the B.E.T. treatment (6). By comparison between the surface area obtained from Equation 1 and the B.E.T. surface, one could determine the surface roughness of the solid powder. The so-called Surface Irregularity Index, having the definition as seen in Equation 2, is introduced.

$$SII = 1 - \frac{A}{A_{BET}} \quad \text{.....(2)}$$

where SII, A, and A_{BET} are Surface Irregularity Index, surface area calculated from geometry of powder size distribution, and surface area obtained from nitrogen adsorption, respectively. The SII values indicate the degrees of surface irregularity which could be compared among different powders due to the dimensionless numbers. This may be an alternative way to characterize the surface morphology of solids.

EXPERIMENTAL

The selected pharmaceutical excipients including unmilled dicalcium phosephate dihydrate (Di-Tab, Rhone-Poulenc Basic Chemical Co.), microcrystalline cellulose (Avicel PH102, FMC Corp.), corn starch (A.E. Staley Mfg. Co.), croscarmellose sodium (Ac-di-sol, FMC Crop.), and sodium starch glycolate (Primojel, GereriChem Corp.) were

Table 1. True density of powders determined by a helium pycnometer.

Material	Density, in g/cc.(s.d.)
Di-Tab	2.7948 (0.0026)
Avicel PH102	1.5520 (0.0045)
Ac-di-sol	1.5900 (0.0010)
corn starch	1.4228 (0.0003)
Primojel	1.5694 (0.0011)

Table 2. The geometric means of sizes and their standard deviations.

Material	$\bar{l}$ (δ_n) in μ.*	Remark
Di-Tab **	60.8(119.05)	14.6(12.58), and 106.9(44.50)
Avicel PH102 **	154.1(152.33)	113.1(88.40), and 443.6(107.27)
Ac-di-sol	71.7(92.34)	skewness
corn starch **	16.0(8.17)	1.3(0.46), and 18.7(8.08)
Primojel	39.7(46.81)	skewness

*The geometric mean calculation is based on the log-normal distribution.
**Bi-modal distribution showing the mean and standard deviation of the individual mode.

employed. All excipients were used as received from the suppliers except as stated in the experiment. The following methods of powder characterization were conducted.

The true density of a powder: The powder density of such an excipient was determined by an automated helium displacement pycnometer (AccuPyc 1330, Micromeritics Instrument Corp.). A sample of from 2 to 6 grams, previously dried for 24 hours at 80 degrees C., was accurately weighed and placed in a sample cell to determine its true volume. With the known weight, the true density was calculated. Three replicates were done for each sample.

Particle size distribution determination: The sizes and size distributions of the selected excipients were determined by a dynamic laser scattering particle size analyzer (Microtrac

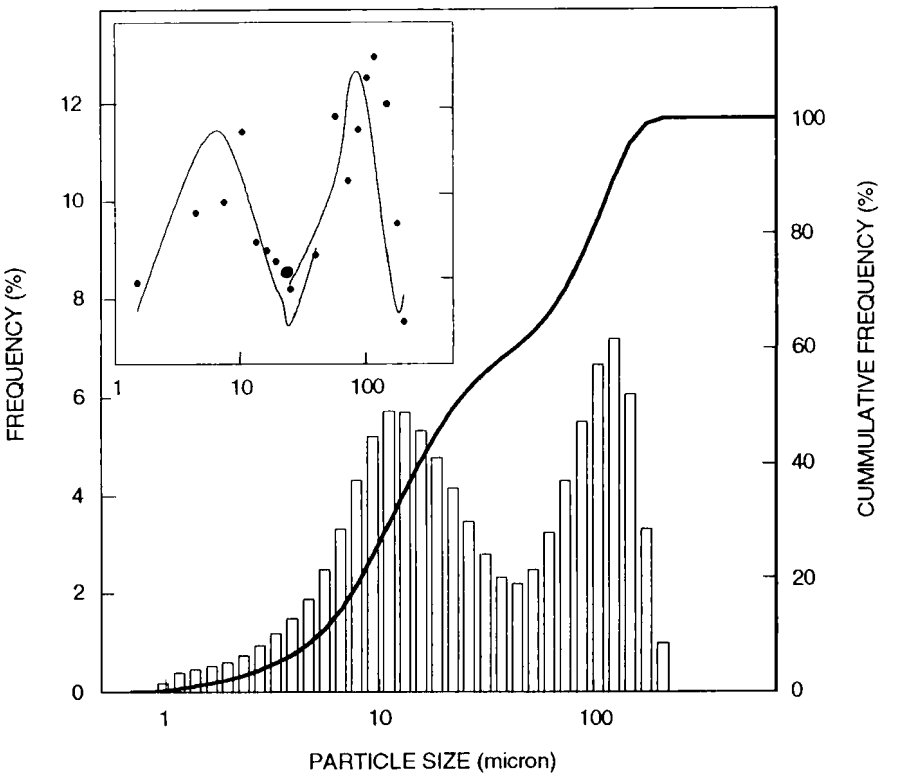

Figure 1. Particle size distribution of Di-Tab powder showing frequency histograms and cumulative plot. (Top-left), The individual log-normal distribution fitting indicated actual data (dots), and predicted lines.

FRA, Leads & Northrup). A sample from 1 to 5 milligrams of powder was suspended in acetone and placed in the small volume cell, a self-contained cell with miniature stirrer motor and agitator. A laser beam was allowed to pass thru the cell and the laser intensity was reduced due to the fact that certain particulate sizes scatter the light. With the aid of computer calculations, the size corresponding to the laser intensity reduction were obtained. The results were expressed as the per cent under-size, i.e., the percentage passing each particular channel adding up to be the particle size distribution.

The surface area determination by nitrogen adsorption: An accurate weight of sample was placed in a sample tube and pretreated by evacuation for 24 hours at 70 degrees C. to remove surface moisture and other contaminants. The surface area of the sample was then

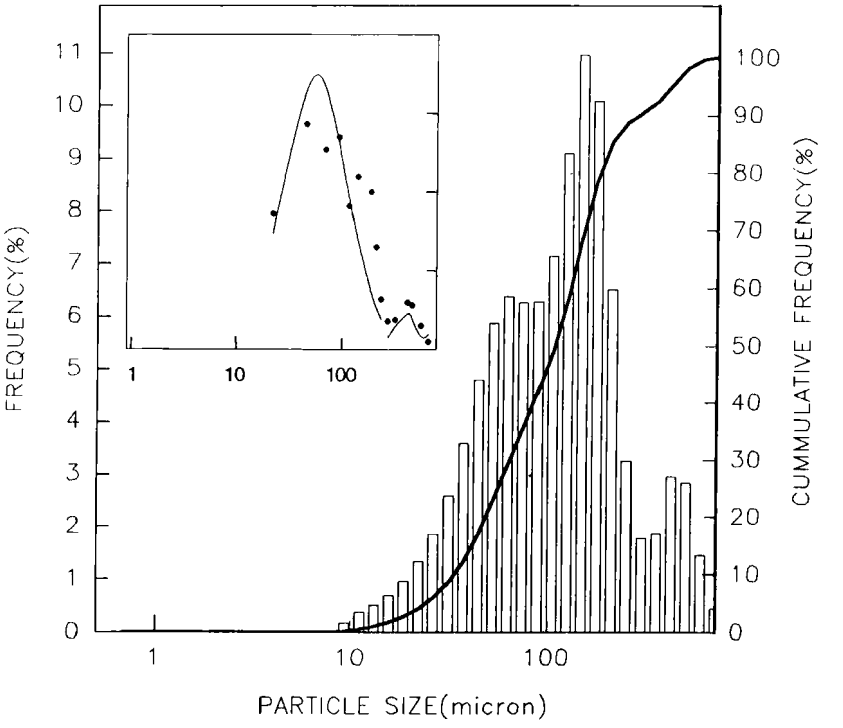

Figure 2. Particle size distribution of Avicel PH102 powder showing frequency histograms and cumulative plot. (Top-left), The individual log-normal distribution fitting indicated actual data (dots), and predicted lines.

determined by the automatic surface area analyzer (Autosorb-1, Quantachrome). Nitrogen was allowed to adsorb on the surface of the powder sample at different equilibrium relative pressure and at 77 K. For each relative pressure, the volume of adsorbed nitrogen was measured and the data were fitted into the B.E.T. equation to determine the surface area.

Microscopic examination: The photomicrographs for each of studied excipients were taken using a Jeol model JMS-6300 scanning electron microscope (Jeol Technics Company, Japan) to examine the surface morphology of a sample. The photomicrographs of the powder samples could confirm the significance of the Surface Irregularity Index.

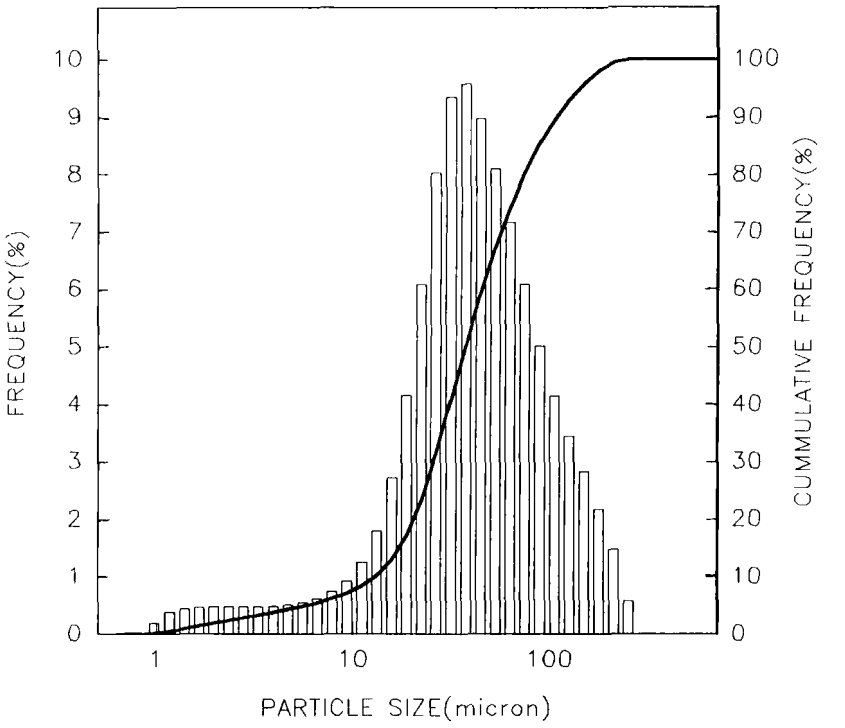

Figure 3. Particle size distribution of Ac-di-sol powder showing frequency histogram and cumulative plot.

RESULTS AND DISCUSSION

The true density of a powder

As seen in Equation 1, the surface area of particles could be calculated if the true density of the powder is known. Table 1 shows the powder densities determined by the automated helium displacement pycnometer.

Particle size distributions

Using a laser scattering method with acetone as a non-swelling medium, the particle size distribution of each of the excipients was determined. The distribution was statistically fitted to the log-normal distribution model (2) to determine the geometrical mean size, and standard deviation ($\bar{1}$, and δ_n) and they are tabulated in Table 2. Compared to the other excipients, the particle distributions of Di-Tab, Avicel PH102 and Ac-di-sol showed somewhat high standard deviations which were affected by their complicated distributions.

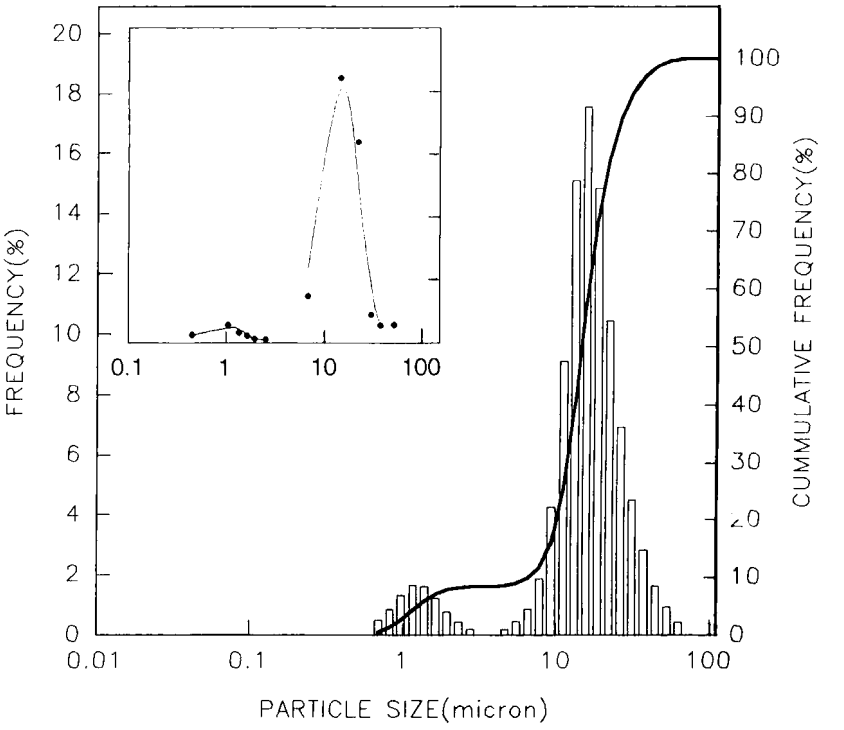

Figure 4. Particle size distribution of corn starch powder showing frequency histograms and cumulative plot. (Top-left), The individual log-normal distribution fitting indicated actual data (dots), and predicted lines.

Figures 1-5 illustrate the powder size distributions of the studied materials. Such a distribution shows a possible complication. At least two modes were noticed in Di-Tab, Avicel PH102, and corn starch particle distributions. These distributions were separated, and individually examined to determine the geometric means (their means and standard deviations were also tabulated in Table 2). As shown in the windows on the top-left of Figures 1, 2, and 4, the individual curve fitting agrees with the powder population data. The results indicated that Di-Tab, Avicel PH102, and corn starch have at least two particle populations.

In addition to the multiple modes of the powder population, the distribution may be skewed. The population of Ac-di-sol powder, for example, exhibited a degree of skewness that could be seen in Figure 3. This is common when non-spherical particle distribution is determined. Ac-di-sol particles are cylindrical in shape. More details in particle morphology are seen by microscopic examination.

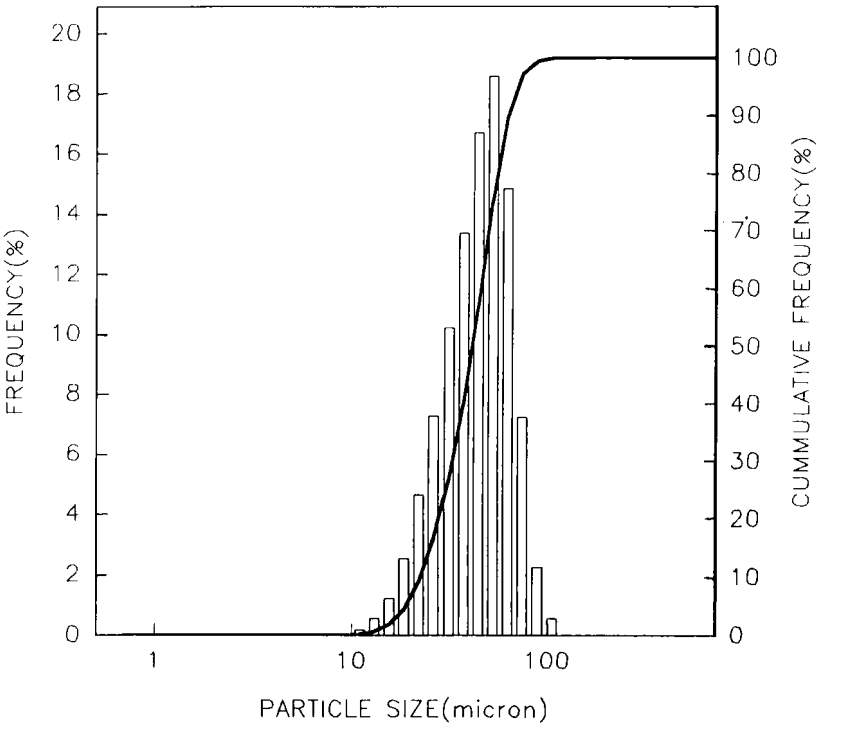

Figure 5. Particle size distribution of Primojel powder showing frequency histogram and cumulative plot.

Table 3. Specific surfaces obtained from B.E.T. treatment.

Material	Specific Surface, m^2/g	*c*-value*	r**
Di-Tab	1.69	95.01	0.9997
Avicel PH102	1.18	97.40	0.9996
Ac-di-sol	0.70	47.34	0.9976
corn starch	0.56	83.06	0.9975
Primojel	0.36	18.51	0.9637

*B.E.T. adsorption constant, **correlation coefficient

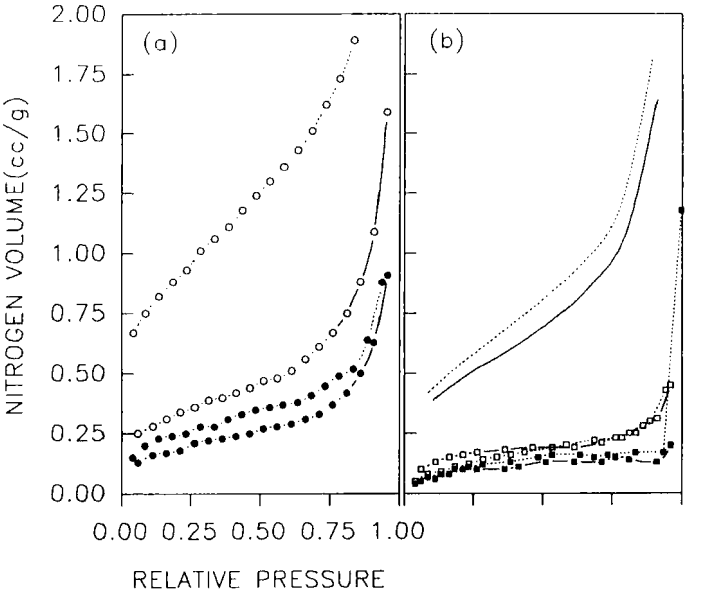

Figure 6. The nitrogen adsorption-desorption isotherms of such excipient powders. Solid and dotted lines represent adsorption and desorption branches, respectively.
Key: (a) Celluloses;
Avicel PH102 (empty circles), and
Ac-di-sol (filled circles).
(b) Starches and Di-Tab;
corn starch (empty squares)
Primojel (filled squares), and
Di-tab (lines).

Table 4. Irregularity Indices of powder materials.

Material	*Shape*	Shape factor*	A_{proj} (m^2/g)	A_{BET} (m^2/g)	*SII*
Di-Tab	*cube*	6.000	0.029	1.69	0.98
Avicel PH102	*cube*	6.000	0.010	1.18	0.99
Ac-di-sol	*rod*	5.536	0.027	0.70	0.96
corn starch	*sphere*	4.836	0.121	0.56	0.78
Primojel	*sphere*	4.836	0.053	0.36	0.85

*Based on the microscopic shape, the values were taken from reference number 4.

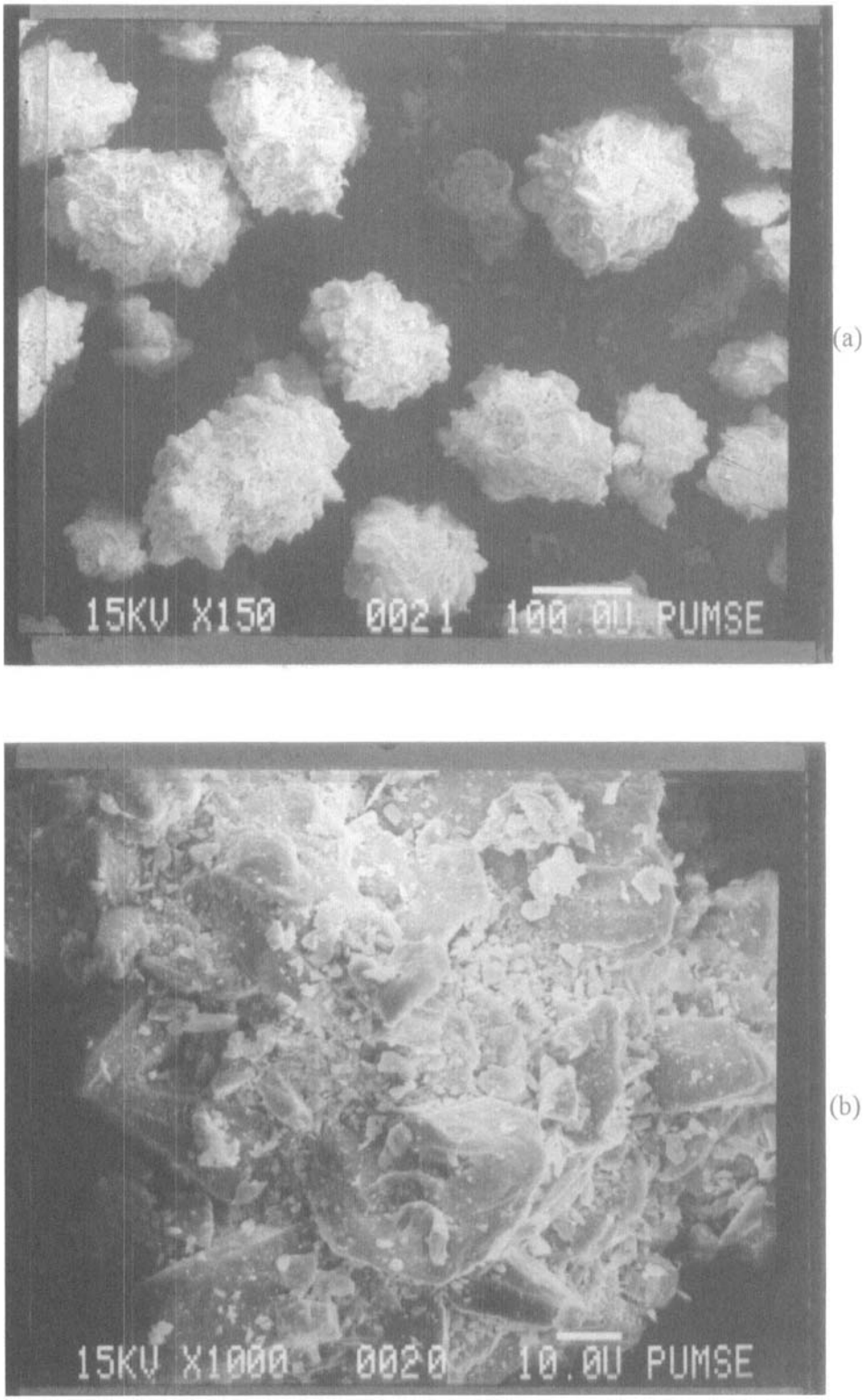

Figure 7. Scanning electron micrographs of Di-Tab powder, (a), × 150; (b), × 1000.

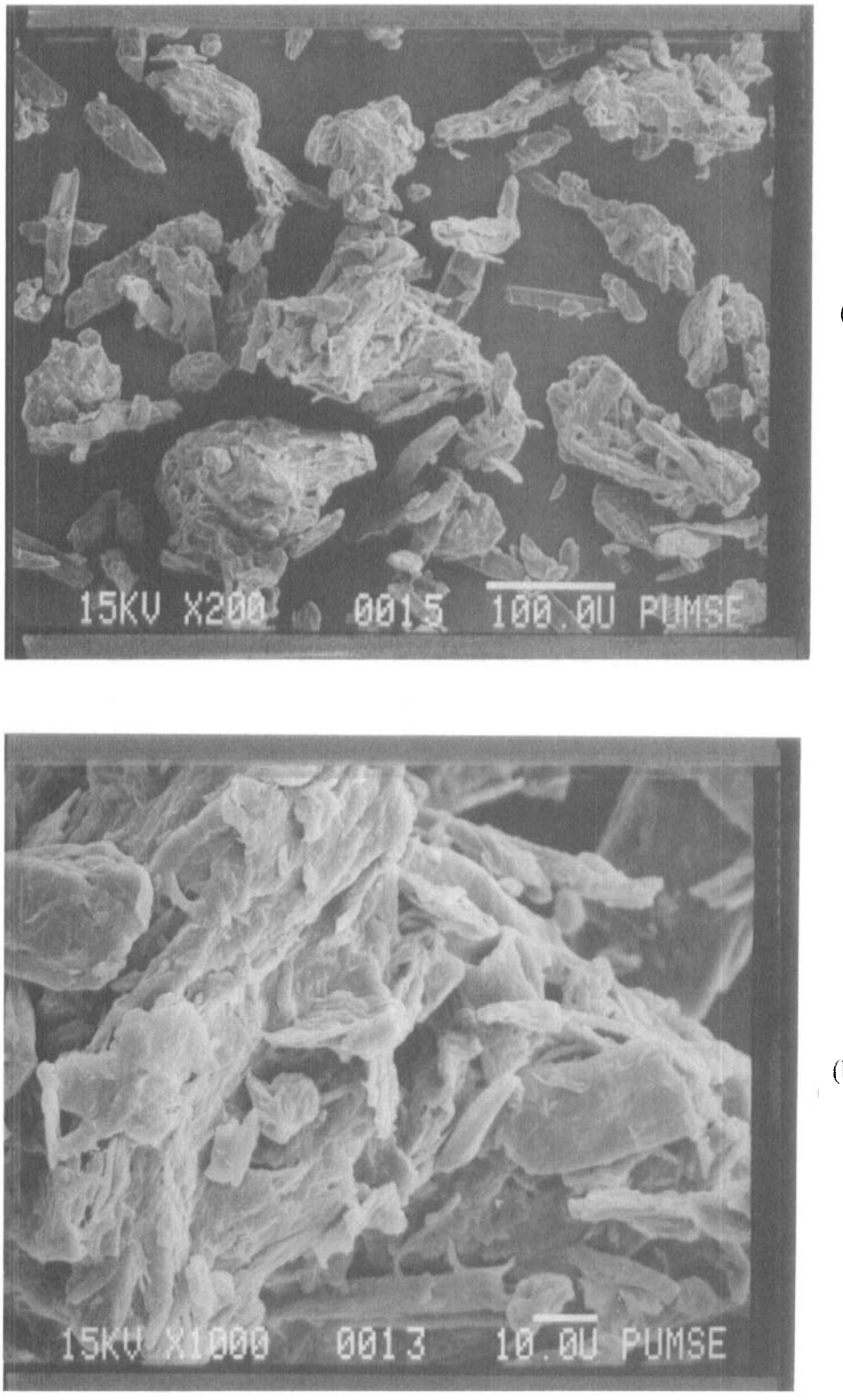

(a)

(b)

Figure 8. Scanning electron micrographs of Avicel PH102 powder, (a), × 200; (b), × 1000.

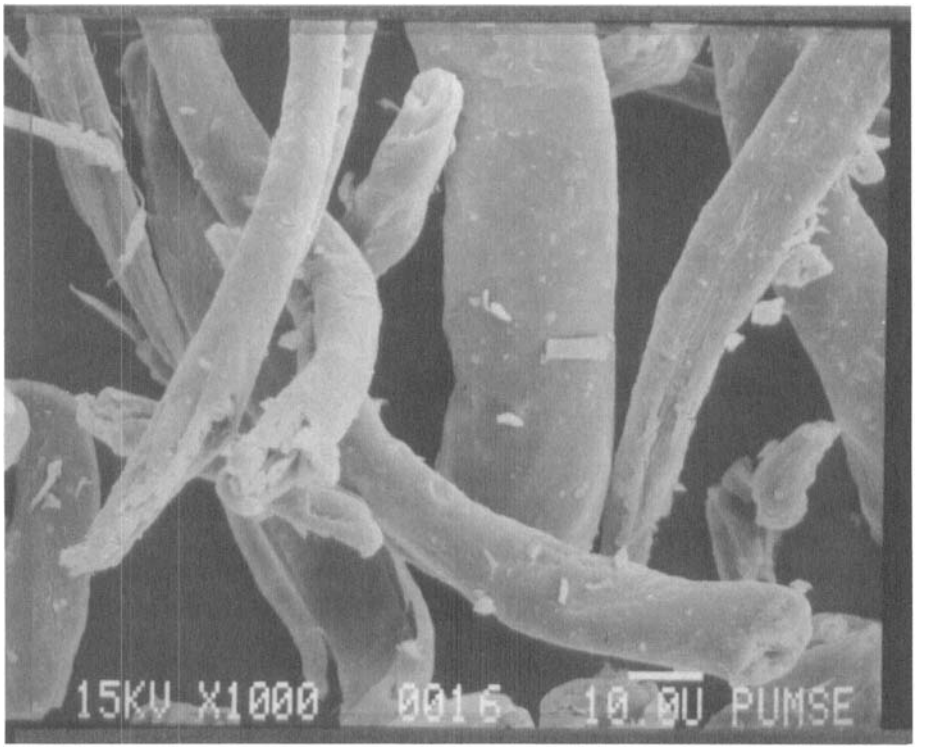

Figure 9.Scanning electron micrograph of Ac-di-sol powder (× 1000).

The surface area determination by nitrogen adsorption

The powder surface area was determined by the nitrogen adsorption. The first five data points of the adsorption branch (relative pressure of 0.05-0.3) of each isotherm were fitted in the B.E.T. model (6) to determine specific surfaces. The surface areas, correlation coefficients of fitting (r), and adsorption constants (*c*-values) for each of the materials are tabulated in Table 3.

As seen in Table 3, the data showed very high statistical correlations. Moreover, adsorption constants indicate the good reliability of the calculated areas using the B.E.T. treatment (2). The adsorption and desorption isotherms of individual powders are illustrated in Figure 6. Each of the samples exhibits type II isotherm that confirms a high adsorption constant.

It is noted from Figure 6 that there is the remaining nitrogen adsorbed on the surface during desorption process. The capillary condensation may take place when the powder is equilibrated at saturation pressure due to the presence of pores on the powder

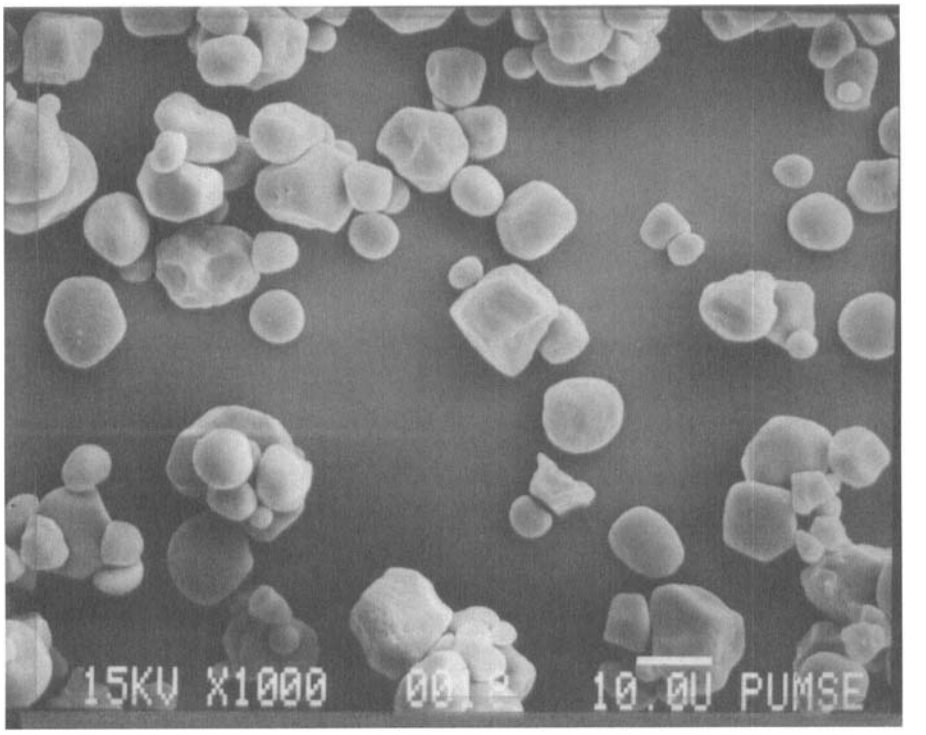

Figure 10.Scanning electron micrograph of corn starch powder (× 1000).

surface. On desorption, the capillaries are emptied by retreat of a meniscus of curvature which is different from adsorption resulting in the hysteresis where the desorption branch lies to the left of the adsorption branch (7). The excipients such as Avicel PH102, Di-Tab, and Ac-di-sol have significant isotherm hystereses (Figure 6). This may be affected by the surface porosity of the excipient.

The Surface Irregularity Index and Microscopic examination

As mentioned earlier, the powder surface area can be estimated from the particle distribution. Disregarding the pores and surface irregularity, the specific surface, which should be called "*projected* surface area", is obtained by using equation 1 with appropriate density shape factor (4). The area related to the pores and surface irregularity is the difference between the areas obtained from nitrogen adsorption and particle distribution. An attempt to indicate powder surface irregularity is made by introducing the so-called the Surface Irregularity Index (*SII*, Equation 2). The projected (A_{proj}) and the B.E.T. surface areas (A_{BET}) , as well as the irregularity indices of studied materials are listed in Table 4.

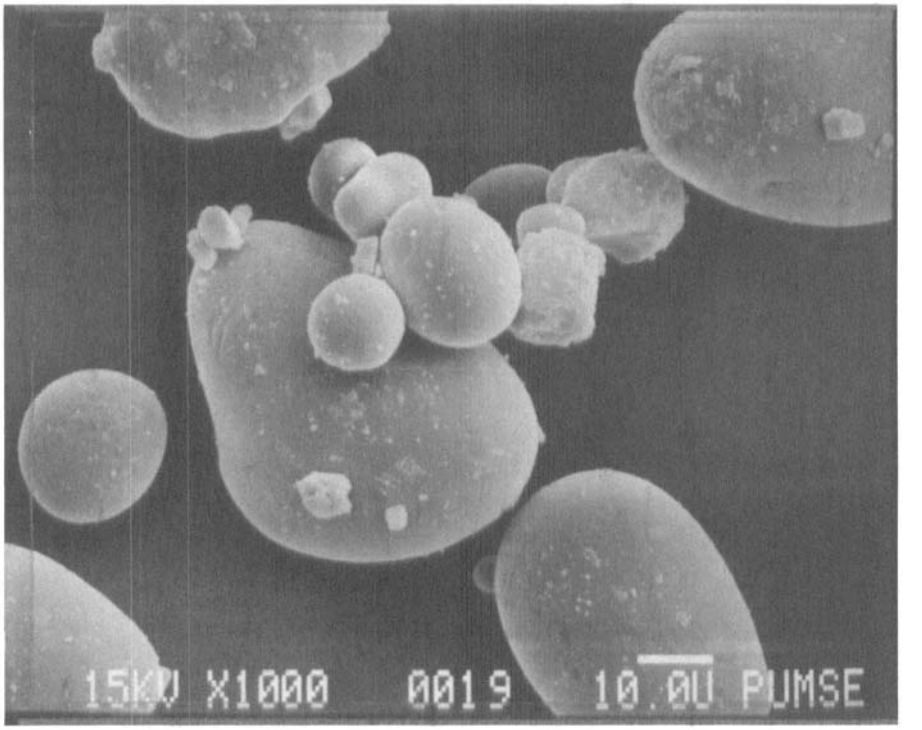

Figure 11. Scanning electron micrograph of Primojel powder (× 1000).

Figures 7-11 show the photomicrographs of the studied excipients. Di-Tab and Avicel PH102 are present in the forms of aggregates. The primary particles agglomerate one another building up the surface porosity which, as seen in Table 4, exhibits high surface irregularity index. On the other hand, corn starch, exhibiting a low value of *SII*, has a somewhat smooth surface compared to other materials in the study (see also the Figures). Ac-di-sol shows somewhat high value in *SII* but the apparent surface morphology rather smooth compared to Di-Tab or Avicel PH102. Exhibiting a cylindrical shape, Ac-di-sol may configure itself as folding filaments when suspended in the particle analyzer medium causing a complication in surface area calculation. Since the projected area calculation is dependent upon the shape factor, the irregularity index comparison between particles with different shapes is difficult. For this study, however, the indices may explain the morphology of powders relating to the microscopic examination.

The surface irregularity reflects the adsorption-desorption isotherm hysteresis due to the capillary condensation in surface pores. The degrees of hysteresis seen in Figure 6 is

consistent with the calculated value of *SII* shown in Table 4. The *SII* may be the alternative approach to determine the surface morphology of solid particles.

CONCLUSION

The surface morphology of a solid powder could be indirectly determined by the Surface Irregularity Index (*SII*) calculation. It is noted that the index is consistent with the microscopic visualization which is a direct method to determine the surface morphology. Moreover, the adsorption-desorption isotherm of each of excipients under study shows the hysteresis which is an evidence of capillary condensation due to the porosity. The degree of hysteresis is also consistent with the *SII* value.

REFERENCES

1. C.G. Schull, and P.E. Elkin, *J. Amer. Chem. Soc.*, 70, 1410 (1948).
2. S.J. Gregg, and K.S. Sing, *Adsorption, Surface Area and Porosity*, second edition, Academic Press, New York, 1982.
3. J.M. Dalla Valle, *Micromeritics*, Pitman Publishing Crop., New York, 1943.
4. J.T. Carstensen, and M. Franchini, *Drug Dev. Ind. Pharm.*, 19(1&2), 85 (1993).
5. *Autiosorb-1: Instruction Manual*, Quantachrome Co., 1990.
6. S. Brunauer, P.H. Emmet, and E. Teller, *J. Amer. Chem. Soc.*, 60, 309 (1938).
7. A.W. Adamson, *Physical Chemistry of Surfaces*, fifth edition, John Wiley & Sons, Inc., New York, 1990.